

Discrete Sources Method for analysis of a light scattering by an air bubble on resist for immersion lithography

Elena Eremina^{a,*}, Thomas Wriedt^b, Yuri Eremin^c

^a*Universitaet Bremen, Badgasteiner Str. 3, 28359 Bremen, Germany*

^b*Institut für Werkstofftechnik, Badgasteiner Str. 3, 28359 Bremen, Germany*

^c*Faculty of Applied Mathematics & Computer Science, Moscow State University, Lenin's Hills 119992 Moscow, Russia*

Abstract

The discrete sources method (DSM) is applied to calculate light scattering by a half-spherical bubble in water on a substrate. For the first time an algorithm which allows the near-field calculation on the base of DSM is presented. Such investigations are important in immersion lithography, as the presence of bubbles on a resist surface decreases image quality. On the base of DSM the numerical algorithm of the near-field calculation is realized. Numerical results for the near-field inside the resist for different depths under the surface are presented.

© 2005 Elsevier Ltd. All rights reserved.

1. Introduction

With need for the further miniaturizing of nanostructures, interest in novel lithography methods increases. Optical lithography is a technique of printing nanostructures onto the surface of a light-sensitive resist using light. It is a part of the quite expensive process of silicon wafers production. Silicon wafers are the core of computer parts, mobile telephones and other electronic devices. The principle difference of immersion lithography from dry one is the presence of an immersion liquid with a refraction index n greater than one (refractive index of air) between the imaging optics and the surface of resist. Among the candidates for such liquids, water appears to be an excellent choice due to its high-transparency at an ultraviolet wavelength of 193 nm, as well as its immediate availability and low processing cost [1]. Water has a high index of refraction, which, combined with low viscosity and absorbance, allows the design of lenses with numerical apertures of 1.2 and greater. The effect of the immersion is twofold. First, the resolution is improved proportionately to n . For water, the index of refraction at $\lambda = 193$ nm is 1.44, improving the resolution significantly from 90 to 64 nm. The second effect of immersion is an increased depth of focus at larger features compared with those that are printable with dry lithography. The development of 193 nm immersion lithography also allows the conservation of much of the existing optical infrastructure. The light source and illumination optics will not be affected. The mask and or pellicle material do not have to be changed. Some modifications to the resist may be required due to liquid-resist interactions and these are currently under investigation. Unfortunately the

*Corresponding author. Tel.: +49 421 218 3583; fax: +49 421 218 5378.

E-mail addresses: eremina@iwt.uni-bremen.de (E. Eremina), thw@iwt.uni-bremen.de (T. Wriedt), eremin@cs.msu.su (Y. Eremin).

immersion lithography as a technique is very sensitive to possible inhomogenities in the immersion liquid. The most dramatic index variations are due to air bubbles formed in the layer because of high surface tension of water. The presence of air bubbles in the immersion layer will degrade the image quality on the resist. Air bubbles can be of nano or micro-size (larger than $3\ \mu\text{m}$). Micro-bubbles usually are not attached to resist surface, like nano-bubbles, but they create a strong shadow under themselves while they are floating in a layer. Nano-bubbles are fixed on the surface and would not move during exposure. Both kinds of bubbles would certainly create a printable defect. Therefore scattering produced by air bubbles in the liquid is of significant concern.

To investigate the influences of bubbles several methods like Mie theory [1] or finite difference time domain (FDTD) have been applied. The Mie theory faces difficulties in the nano-bubble case due to half-spherical bubble's shape and presence of water layer and resist. Mostly the FDTD is used to investigate this effect. But the FDTD is a rather time-consuming method, as it is based on volume discretization. Therefore we chose the discrete sources method (DSM), which allows to take into account analytically all the interaction between bubble and resist surface. Besides, the DSM makes use of the bubble symmetry, which sufficiently reduces calculation time. One of the advantages the DSM gives is the possibility to estimate an a posteriori error of the numerical results via surface residual calculation [2].

2. Theory

An air-bubble situated on the resist substrate in water is plotted in Fig. 1. We will assume that the bubble has a half-spherical shape and the hydraulic pressure of water is ignored. Then we consider a half-spherical bubble with an interior domain D_i and smooth boundary ∂D deposited above the plane interface Σ . We denote the prism domain by D_1 and the ambient domain exterior to the particle filled with water by D_0 . Let us introduce a Cartesian coordinate system $Oxyz$ by choosing its origin O at the intersection point of the axis of symmetry of the particle and the plane Σ . The z -axis coincides with the axis of symmetry and is directed into domain D_0 so, that the plane $z = 0$ coincides with the Σ plane. We assume that the exciting field $\{\mathbf{E}^0, \mathbf{H}^0\}$ is a plane wave propagating from the area D_0 at the angle $\pi - \theta_0$ with respect to the z -axis (Fig. 1). Then the mathematical statement of the scattering problem can be formulated in the following form:

$$\begin{aligned} \nabla \times \mathbf{H}_\zeta &= jk\varepsilon_\zeta \mathbf{E}_\zeta, & \nabla \times \mathbf{E}_\zeta &= -jk\mu_\zeta \mathbf{H}_\zeta & \text{in } D_\zeta, \zeta = 0, 1, i, \\ \mathbf{n} \times (\mathbf{E}_i - \mathbf{E}_0) &= 0, & \mathbf{n} \times (\mathbf{H}_i - \mathbf{H}_0) &= 0 & \text{at } \partial D, \\ \mathbf{e}_z \times (\mathbf{E}_0 - \mathbf{E}_1) &= 0, & \mathbf{e}_z \times (\mathbf{H}_0 - \mathbf{H}_1) &= 0 & \text{at } \Sigma, \end{aligned} \quad (1)$$

and radiation conditions for the scattered field at infinity.

Here, \mathbf{n} is the outward unit normal vector to ∂D , $k = \omega/c$, $\text{Im } \varepsilon_\zeta, \mu_\zeta \leq 0$ (time dependence for the fields is chosen as $\exp\{j\omega t\}$) and the particle surface is smooth enough $\partial D \subset C^{(1,\infty)}$. Field $\{\mathbf{E}_\zeta, \mathbf{H}_\zeta\}$ stands for the total

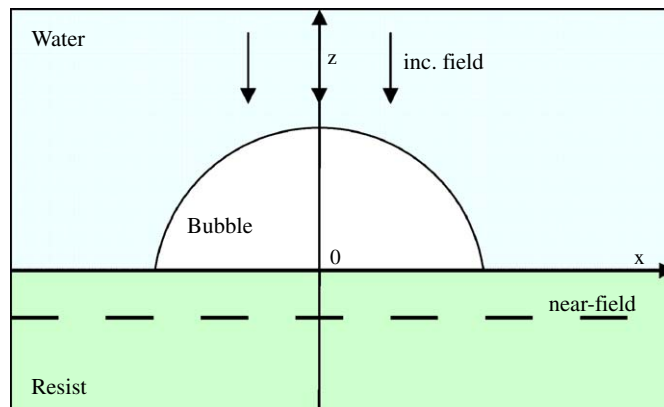


Fig. 1. Problem geometry.

field in corresponding domain D_ζ . Note that the total field in D_0 is a superposition of the exciting field and the scattered one.

In the frame of DSM first the plane wave $\{\mathbf{E}^0, \mathbf{H}^0\}$ scattering problem on a layered interface is solved. The resulting field $\{\mathbf{E}_\zeta^0, \mathbf{H}_\zeta^0\}$, $\zeta = 0, 1$ satisfies the transmission condition of the plane Σ . Next step is to construct an approximate solution $\{\mathbf{E}_\zeta^s, \mathbf{H}_\zeta^s\}$ for the scattering fields in the D_ζ , $\zeta = 0, 1$ and a total field inside a bubble following the DSM concept [2]. An approximate solution is constructed as a finite linear combination of the fields of discrete sources (DS) (dipoles and multipoles) deposited in a supplementary domain. Under these conditions the representation satisfies Maxwell equations in D_ζ , $\zeta = 0, 1, i$, transmission conditions at the interface and infinity conditions. The unknown amplitudes of DS are to be determined from the transmission conditions at the particle boundary, which can be rewritten as

$$\mathbf{n} \times (\mathbf{E}_i - \mathbf{E}_0^s) = \mathbf{n} \times \mathbf{E}_0^0, \quad \mathbf{n} \times (\mathbf{H}_i - \mathbf{H}_0^s) = \mathbf{n} \times \mathbf{H}_0^0 \quad \text{at } \partial D. \quad (2)$$

So the boundary-value scattering problem under investigation is reduced to the solution of an approximation problem enforced at an obstacle surface [2].

We will consider an axial symmetrical particle. In this case the system of lowest order multipoles distributed over the axis of symmetry can be applied to construct an approximate solution [3]. As a consequence the surface approximating problem can be reduced to a number of one-dimensional problems enforced at the particle generatrix. The approximate solution will be constructed taking into account not only the rotational symmetry of the obstacle, but also the polarization of an external excitation as well.

In case of P polarized light the exciting field accepts the following form:

$$\begin{aligned} \mathbf{E}_0^0 &= \mathbf{e}_x \cos \theta_0 (\chi^- - R_P \chi^+) + \mathbf{e}_z \sin \theta_0 (\chi^- + R_P \chi^+), \\ \mathbf{H}_0^0 &= -\mathbf{e}_y (\chi^- + R_P \chi^+), \end{aligned}$$

$$\chi^- = \exp\{-i\eta_0(x \sin \theta_0 - z \cos \theta_0)\}, \quad \chi^+ = \exp\{-i\eta_0(x \sin \theta_0 + z \cos \theta_0)\}.$$

Here $n_{0,1} = \sqrt{\epsilon_{0,1} \mu_{0,1}}$ is associating refractive indexes of D_0 , θ_0 is an incident angle and the reflection coefficient R_P can be written as

$$R_P = \frac{n_1 \cos \theta_0 - n_0 \cos \theta_1}{n_1 \cos \theta_0 + n_0 \cos \theta_1}.$$

To take the polarization of the external excitation into account we use a linear combination of electrical and magnetic multipoles. For this we need special vector potentials. In case of P-polarization of the plane wave the representation for vector potentials in a cylindrical coordinate system can be represented as

$$\mathbf{A}_{mn}^{e,0}(\eta, z_n) = \{G_m^c(\eta, z_n) \cos(m+1)\varphi; -G_m^s(\eta, z_n) \sin(m+1)\varphi; -g_{m+1}(\eta, z_n) \cos(m+1)\varphi\},$$

$$\mathbf{A}_{mn}^{h,0}(\eta, z_n) = \{G_m^h(\eta, z_n) \sin(m+1)\varphi; G_m^c(\eta, z_n) \cos(m+1)\varphi; -g_{m+1}(\eta, z_n) \sin(m+1)\varphi\},$$

$$\mathbf{A}_{0n}^{e,h,0}(\eta, z_n) = \{0; 0; G_0^{h,e}(\eta, z_n)\}.$$

Here the corresponding azimuthal Fourier harmonics of the Green tensor components in water can be presented as Weyl–Sommerfeld integrals [2]:

$$G_m^{e,h}(\eta, z_n) = \frac{k_0}{i} h_m^{(2)}(k_0 R_{\eta z_n}) \left(\frac{k_0 \rho}{R_{\eta z_n}} \right)^m + \int_0^\infty J_m(\lambda \rho) v_{11}^{e,h}(\lambda, z_n) \exp\{-\eta_0 z\} \lambda^{1+m} \partial \lambda,$$

$$g_m(\eta, z_n) = \int_0^\infty J_m(\lambda \rho) v_{31}(\lambda, z_n) \exp\{-\eta_0 z\} \lambda^{1+m} \partial \lambda, \quad R_{\eta z_n}^2 = \rho^2 + (z - z_n)^2.$$

Here $h_m^{(2)}$ is a spherical Hankel function, point $\eta = (\rho, z)$, belongs to the semi-plane $\varphi = 0$, ρ, φ, z are the coordinates of a cylindrical coordinate system, which origin coincides with 0-point at Fig. 1. $\{z_n\}_{n=1}^\infty$ is a dense set of discrete source points distributed over a segment $\Gamma_z^0 \in D_i$ at the axis of symmetry, and

$v_{11}^{e,h}(z, z_n, \lambda)$, $v_{31}(z, z_n, \lambda)$ are the corresponding spectral functions which are given by

$$v^e(\lambda, z_n) = \frac{\mu_1 \eta_0 - \mu_0 \eta_1}{\mu_1 \eta_0 + \mu_0 \eta_1} \frac{1}{\eta_0} \exp\{-\eta_0 z_n\},$$

$$v_{11}^h(\lambda, z_n) = \frac{\varepsilon_1 \eta_0 - \varepsilon_0 \eta_1}{\varepsilon_1 \eta_0 + \varepsilon_0 \eta_1} \frac{1}{\eta_0} \exp\{-\eta_0 z_n\}; \quad z_n \geq 0,$$

$$v_{31}(\lambda, z_n) = \frac{2(\mu_1 \varepsilon_1 - \mu_0 \varepsilon_0)}{(\mu_1 \eta_0 + \mu_0 \eta_1)(\varepsilon_1 \eta_0 + \varepsilon_0 \eta_1)} \exp\{-\eta_0 z_n\},$$

where $\eta_\zeta^2 = \lambda^2 + k_\zeta^2$, $k_\zeta^2 = k^2 \varepsilon_\zeta \mu_\zeta$, $\zeta = 0, 1$ in the paper we will use indices 0 for the water area and 1 for the area inside resist, we will also use index i for area inside the bubble and e for outer area. The vector potentials for the field representation inside a bubble have a form

$$\mathbf{A}_{mn}^{e,i}(\eta, z_n) = \{J_m^i(\eta, z_n) \cos(m+1)\varphi; -J_m^i(\eta, z_n) \sin(m+1)\varphi; 0\},$$

$$\mathbf{A}_{mn}^{h,i}(\eta, z_n) = \{J_m^i(\eta, z_n) \sin(m+1)\varphi; J_m^i(\eta, z_n) \cos(m+1)\varphi; 0\},$$

$$\mathbf{A}_{0n}^{e,h,i}(\eta, z_n) = \{0; 0; J_0^i(\eta, z_n)\},$$

where $J_m^i(\eta, z_n) = j_m(k_i R_{\eta z_n})(\rho/R_{\eta z_n})^m$, j_m are the spherical Bessel functions.

So the approximate solution taking into account P-polarization of the plane wave and axial symmetry of the particle can be represented in the form

$$\begin{aligned} \mathbf{E}_N^\zeta &= \sum_{m=0}^M \sum_{n=1}^{N_\zeta^m} \left\{ p_{mn}^\zeta \frac{\mathbf{j}}{k \varepsilon_\zeta \mu_\zeta} \nabla \times \nabla \times \mathbf{A}_{mn}^{e,\zeta} + q_{mn}^\zeta \frac{\mathbf{j}}{\varepsilon_\zeta} \nabla \times \mathbf{A}_{mn}^{h,\zeta} \right\} + \sum_{n=1}^{N_0^\zeta} r_n^\zeta \frac{\mathbf{j}}{k \varepsilon_\zeta \mu_\zeta} \nabla \times \nabla \times \mathbf{A}_{0n}^{e,\zeta}, \\ \mathbf{H}_N^\zeta &= \frac{\mathbf{j}}{k \mu} \nabla \times \mathbf{E}_N^\zeta, \quad \zeta = 0, i. \end{aligned} \quad (3)$$

To ensure convergence of the approximate solution to the exact one it is sufficient to provide the completeness of the system of distributed multipoles which are used for the approximate solutions representation. The scattering from the S-polarized plane wave can be analyzed in the same manner [4].

Let us shortly describe the numerical algorithm. The approximate solution (3) satisfies Maxwell's equations and radiating conditions at infinity. As the approximate solution satisfies all the conditions of the original scattering problem, except the boundary conditions, the unknown vector of amplitudes of DS

$$\mathbf{p}_m = \{p_{mn}^{e,i}, q_{mn}^{e,i}, r_n^{e,i}\}_{n=1}^{N_{e,i}^m},$$

is to be determined from the boundary conditions at the particle surface. The indices i, e here belong to DS which are used for internal and external fields representation. As the DS are distributed on the symmetry axis of the particle, the approximate solution is a finite linear combination of Fourier harmonics with respect to the φ angle variable. The plane wave excitation can also be resolved into a Fourier series with respect to the φ angle variable [3]. So, one can reduce the surface approximation problem enforced at the particle surface to a sequence of one-dimensional problems at the particle generatrix. To solve this problem the general matching-point technique [2] is used. For the near field calculations inside the resist the spectral functions of light refracted by the interface are used.

3. Results

The intensity of the scattered light and the intensity of the incident field at $z = 0$ level can be presented in form

$$I^s(M) = \frac{|\mathbf{E}_1^{s,S}|^2 + |\mathbf{E}_1^{s,P}|^2}{2}, \quad I^0(M) = \frac{|\mathbf{E}_0^{0,S}|^2 + |\mathbf{E}_1^{0,P}|^2}{2}.$$

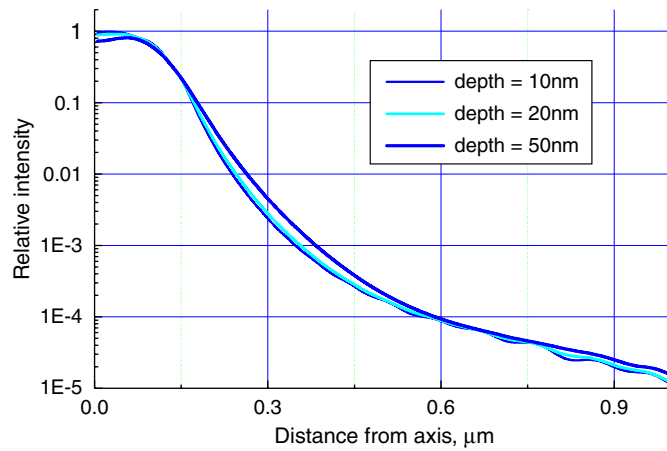


Fig. 2. Intensity of scattered light for an air-bubble of $D = 300$ nm on resist surface for different depths of near-field d .

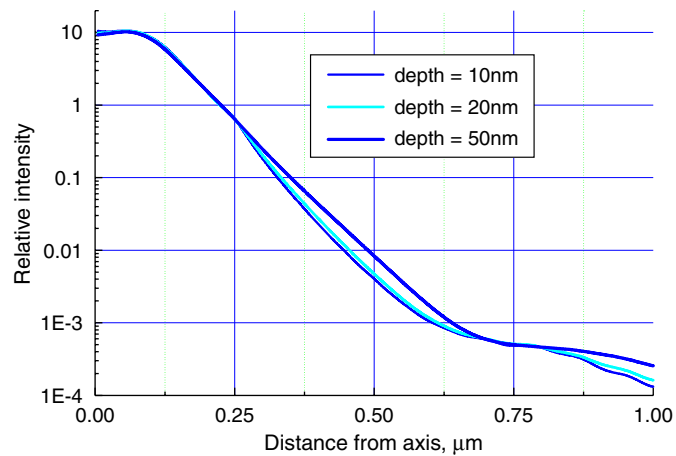


Fig. 3. Intensity of scattered light for an air-bubble of $D = 500$ nm on resist surface for different depths of near-field d .

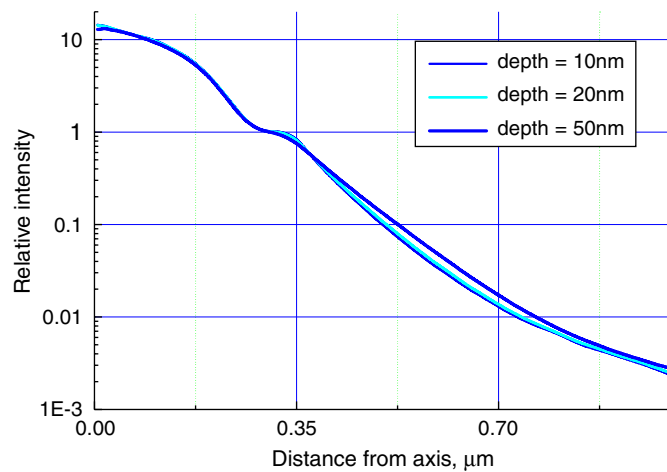


Fig. 4. Intensity of scattered light for an air-bubble of $D = 700$ nm on resist surface for different depths of near-field d .

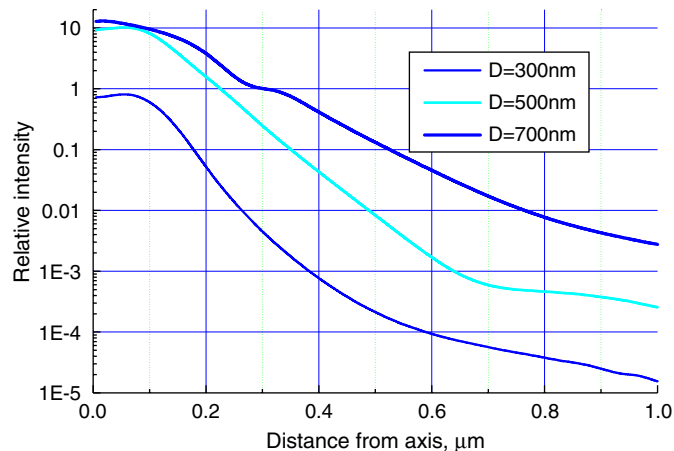


Fig. 5. Intensity of scattered light for an air-bubbles of different diameters D on resist surface, depths of near-field $d = 50$ nm.

In the paper, we calculate the relative scattered intensity which can be written as $I = I^s(\rho, 0, d)/I^0(\rho, 0, 0)$. The relative intensity is calculated inside a resist for different depth (d) of a near-field under the surface. The incident wavelength in water is $\lambda_w = 137.85$. The refractive index of water is $n_w = 1.4$, the resist refractive index is $n_r = 1.7 - 0.007i$, the bubble refractive index is $n_b = 1.0$. In Fig. 2 the scattered intensity versus the distance from the axis of symmetry of the bubble is presented for bubble's diameter $D = 300$ nm for different depth under the resist surface. In Figs. 3, 4 the corresponding results for $D = 500$ and 700 nm are presented. The results show that the intensity of the scattered light achieves its maximum value on the distance from axis not exceeding bubble's radius. Then the intensity rapidly decreases with increasing distance from the axis. Fig. 5 presents comparative results for different bubble diameters but fixed depths of $d = 50$ nm. Bigger bubbles show higher scattering, but their influence is considerable also mainly under the bubble itself. But under a bubble the intensity of scattered light can be much higher than the incidence intensity on the resist surface.

4. Conclusion

In this paper light scattering by an air bubble on a plane interface is investigated. The numerical results obtained on the base of DSM are presented. It was shown, that the influence of the bubble is especially strong in the area under a bubble. In the paper only the scattered near-field has been computed, the total near-field is the aim of our future investigations.

Acknowledgment

We would like to acknowledge support of this work by Deutsche Forschungsgemeinschaft (DFG).

References

- [1] Fan Y, Lafferty N, Bourov A, Zavyalova L, Smith BW. Study of air bubble induced light scattering effect on image quality in 193 nm immersion lithography. In: Proceedings of SPIE 5377, 2004.
- [2] Eremin YA. The method of discrete sources in electromagnetic scattering by axially symmetric structures. J Commun Technol Electronics 2000;45(S2):269–80.
- [3] Eremina EY, Sveshnicov AG. Analysis of light scattering by particle inside a layer via discrete sources method. Moscow university physics bulletin, vol. 1. Allerton Press, 1999. p. 8–16.
- [4] Doicu A, Eremin Y, Wriedt T. Acoustic and electromagnetic scattering analysis using discrete sources. London: Academic Press; 2000.